科学通报 2017 年 第 62 卷 第 33 期: 3829 ~ 3837
进 展
《中国科学》杂志社
SCIENCE CHINA PRESS

二维半导体材料的生长和光电性能研究

黎博, 魏钟鸣*

中国科学院半导体研究所, 半导体超晶格国家重点实验室, 北京 100083
* 联系人, E-mail: zmwei@semi.ac.cn

2017-04-22 收稿, 2017-06-14 修回, 2017-06-14 接受, 2017-09-06 网络版发表
国家自然科学基金优秀青年科学基金(61622406)资助

摘要 二维过渡金属硫族化合物纳米材料由于是不同带隙的半导体, 同时有些在地球上储量丰富, 受到人们广泛的关注. 在本文中, 介绍了用于二维材料场效应晶体管制备的光刻图形转移技术. 该方法可以低成本、简单、有效地获得晶体管, 同时对二维材料的损伤较小, 可以获得高性能的二维材料晶体管; 其次, 介绍了Co掺杂MoS_2双层纳米片的生长及电学输运研究, 可以通过控制生长过程中硫的浓度来改变纳米片的形貌, 随着温度的升高, 最终可以获得CoS_2/MoS_2六边形结构, 电学测试表明Co掺杂MoS_2双层纳米片显n型, 而CoS_2/MoS_2六边形结构具有很高的电导率; 还介绍了垂直双层SnS_2/MoS_2异质结的气相生长及光电性能研究, 这种异质结具有很大的带阶, 能带结构呈现Ⅱ型, 在异质结区域, 出现了强烈的光致发光谱淬灭, 这种异质结与相应的单体材料相比, 具有增强的光电性能. 最后, 对二维材料的未来研究进行一些展望.

关键词 二维半导体, 二硫化钼, 气相生长, 光电器件

自从2004年, 石墨烯(graphene)被英国曼彻斯特大学的Novoselov等人[1]发现以来, 二维材料就受到了人们的广泛关注. 二维材料层内以强烈的共价键结合, 层与层之间以较弱的范德瓦尔斯(范德华)力结合, 所以容易剥离. 二维材料可以由单元系或多元系构成, 比如单元系有石墨烯、硅烯、黑磷等. 多元系有硫化钼(MoS_2)、硫化钨(WS_2)等(图1)[2~5]. Graphene是由二维sp^2杂化碳薄片命名的. 单层石墨烯在实验上的实现, 导致了很多原创性的工作出现: 石墨烯的双极性场效应、室温的量子霍尔效应、超级高的载流子迁移率以及首次探测到单分子吸附等[1,6]. 石墨烯的这些优异的性能在未来的研究中、在热导和电导增强的复合物、传感器以及太阳能透明电极等方面应用有巨大潜力. 但是由于石墨烯是本征零带隙的, 这就限制了其在逻辑电路的发展. 二维过渡金属硫族化合物(TMDs)具有化学式MX_2 (M=Mo, W等, X=S, Se, Te), 单层MX_2是由两层X夹着一层M的三明治结构组成的. M-X键是较强的共价键, 层与层之间的X-X键是较弱的范德瓦尔斯键. 由于层间耦合作用的不同, 不同层数的MX_2会表现出明显不同的能带结构和物理性质. TMDs具有不同的能带结构, 比如有金属、半导体、绝缘体[2]. 其中的半导体材料, 如MoS_2, WS_2等, 能带结构强烈依赖层数变化, 随着层数的增加, 带隙会逐渐变小[7~11]. 同时这些材料展现了良好的电学和光电性能, 在未来的光电探测、逻辑电路等方面有很大的发展潜力[7,12].

探究二维材料新的性质和将二维材料应用到现代工业中一直是二维材料研究的主题. 当前二维材料的研究主要分为3个方向: 新型二维材料、二维掺杂材料、二维异质结. 新的二维材料可能会有新的性能, 拓展二维材料的研究领域[13]. 二维掺杂材料可以用于调控带隙, 得到不一样的光电性能等[14~22].

引用格式: 黎博, 魏钟鸣. 二维半导体材料的生长和光电性能研究. 科学通报, 2017, 62: 3829–3837
Li B, Wei Z M. Growth and optoelectronic property of two-dimensional semiconductors (in Chinese). Chin Sci Bull, 2017, 62: 3829–3837, doi: 10.1360/N972017-00431

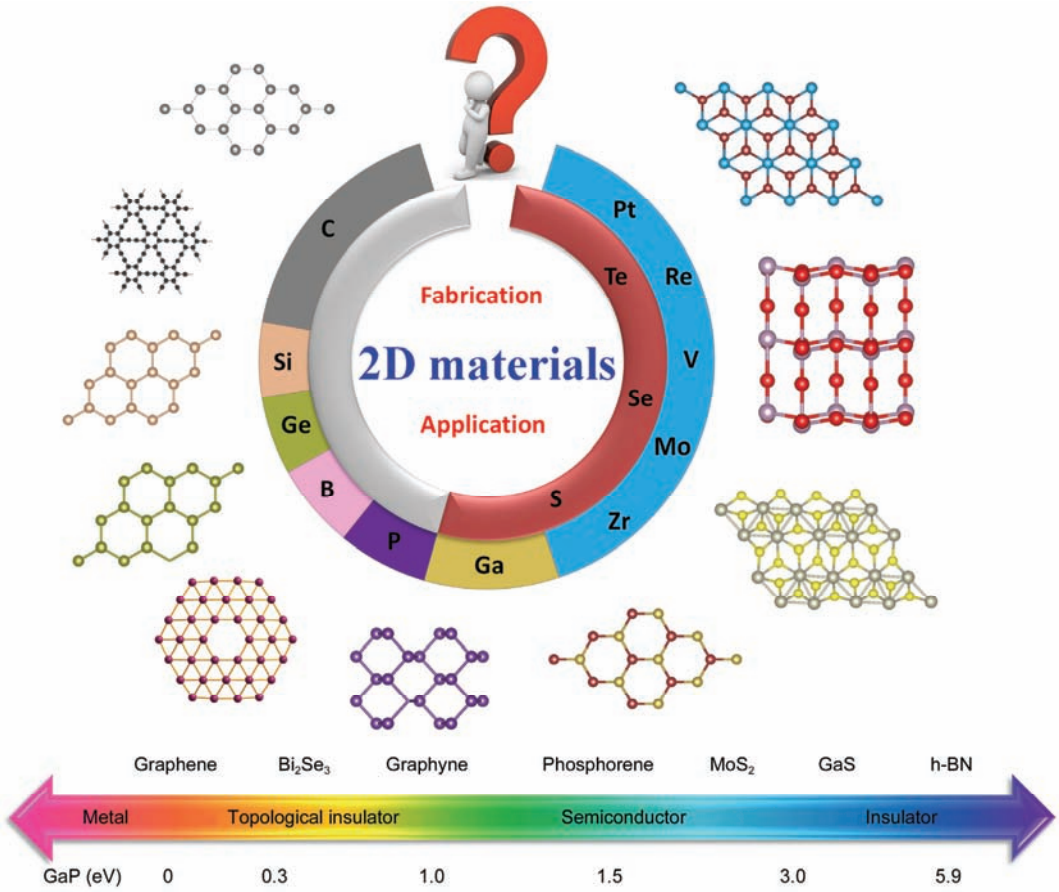

图 1 (网络版彩色)典型二维材料结构与带隙示意图

Figure 1 (Color online) Schematic of various structures and band gaps of two-dimensional materials

二维范德华异质结在高速电路、发光二极管、光伏产业等方面有重要应用[23~37]. 同时, 二维半导体材料由于具有原子层厚度, 器件制备的工艺和方法对其电学性能影响较大, 所以改进工艺、摸索新方法对于提高二维材料的电学和光电性能是至关重要的. 本文主要介绍近期基于二维材料的器件制备发展出的光刻图形转移(photolithographic-pattern transfer)技术[38], 以及通过化学气相法制备的$Co_{0.16}Mo_{0.84}S_2$掺杂二维材料[39], 还有化学气相法直接生长的二维硫化锡/硫化钼(SnS_2/MoS_2)双层垂直异质结[40].

1 光刻图形转移技术

传统的用于制备微纳器件的方法有电子束光刻(EBL)、紫外光刻(UVL)、掩膜热蒸发等. EBL能根据样品的形貌做出合适的器件, 而UVL则可以很方便地大面积地制备器件, 但这两者一般设备昂贵, 工艺复杂. 掩膜热蒸发工艺简单, 操作方便, 但是制备精巧的器件比较困难. 对于原子层厚度的二维材料, 由于蒸金的时候, 很容易破坏平面内的共价键, 从而对材料的性能造成影响. 如何最大限度地减少对材料的破坏, 同时工艺简单, 这是二维材料微纳器件制备研究的主题之一. 基于这个目的, 我们发展了一种光刻图形转移法来制备二维材料微纳器件. 该方法操作简单, 成本低廉, 而且对二维材料损伤较小[38]. 这种方法分为两步, 第一步是电极制备, 第二步是转移电极到样品上. 电极是通过类似光刻的方法制备的, 只是没有用到光刻机, 光刻胶是能与可见光反应的, 光源可以是太阳光、氙灯、显微镜灯等, 尽量选取平行度高的光, 同时曝光时间和显影时间要摸索好, 这之后就蒸金、去金(图2(a)). 可以用这种方法获得大量的形状不一的电极(图2(c)), 电极的最短沟道可到2 μm. 电极制好后, 就用PMMA(polymethyl methacrylate)转移到样品, 先将PMMA旋涂到电极上, 然后用NaOH腐蚀掉SiO_2, 沾有电极的PMMA就能被转

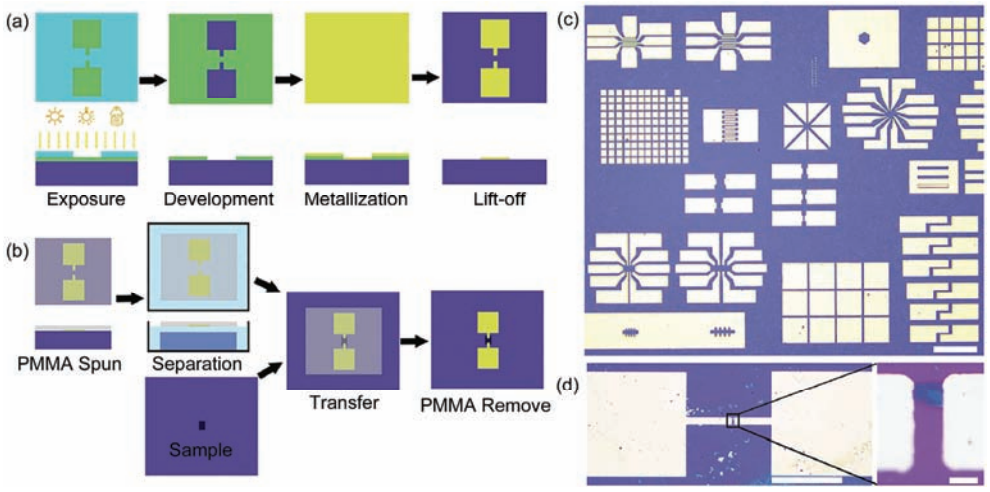

图 2 (网络版彩色)光刻图形转移法的介绍. (a) 电极制备过程示意图; (b) 转移电极到样品上的过程示意图; (c) 用卤光灯曝光获得的电极的图片; (d) 用这种方法得到的器件图

Figure 2 (Color online) Illustration of photolithographic-pattern-transfer method. (a) Exposure and patterning, in which sunlight, incandescent light bulb, fluorescent lamp, and so on, could be employed as the light source; (b) transferring and aligning electrodes with the sample; (c) image of Au electrodes on SiO_2/Si substrate by using a straight halogen light source; (d) typical image of final device from (b)

移到样品上, 最后用丙酮去除PMMA, 200℃左右退火器件, 去除残留的水和PMMA. 用这种方法获得的一个典型的器件如图2(d)所示.

我们还认真比对了用这种方法与用EBL和UVL做出二维材料的器件的性能. 发现本文这种方法做出的器件性能不比EBL和UVL的差, 有些甚至更好. 究其原因, 就是这种方法没有在样品上进行涂胶、紫外或电子束曝光、去胶等步骤, 而且也不是直接在样品上面蒸金的, 只是在样品上覆盖一层PMMA, 然后用丙酮去掉, 最大程度地减少了对二维材料的损害. 文献[41]中也报道了通过制备二维异质结来避免镀金电极对二维材料的破坏. 同时, 还发现, 可以通过调整旋涂的转速来控制PMMA的厚度, 在转移电极的时候, 由于PMMA是绝缘材料, 将电极翻转过来, 就可以非常简单地获得顶栅压电极. 除了制备单个的二维材料器件, 还用这种方法制备了二维异质结器件, 测试出的电学性能也很好. 本文发展的这种光刻图形转移方法非常适用于实验室中二维材料的器件制备.

2 Co掺杂MoS_2双层纳米片的制备及电学研究

与石墨烯的零带隙不同, 大部分单层的二维TMDs材料具有直接带隙, 而且随着厚度的变化, 带隙也会变化[8]. 调节这些材料的带隙对于他们的电学和光电学应用是极为有利的. 在二维TMDs中, 大部分都具有类似的晶体结构, 还有些具有相近的晶格常数, 比如MoS_2, WS_2, $MoSe_2$和WSe_2具有相同的三明治的结构, 其中MoS_2和WS_2的晶格常数分别是0.315和0.316 nm, $MoSe_2$和WSe_2的晶格常数都是0.329 nm. 晶格常数匹配使得合金成为可能, 而合金可以改变单一材料的带隙, 所以通过制备二维TMDs的合金来调控带隙是当前二维材料掺杂的一个热点[14,17,18,21]. 同时掺杂其他的原子也可能获得不一样的电学和光电性能, 比如在MoS_2中掺杂Nb能导致n型导电向p型导电的转变[42]; 在SnS_2中掺杂Se, 则会获得增强的光电性能以及可调控的迁移率[43,44]. 理论计算预测, Mn, Fe, Co等掺杂的TMDs可能具有磁性, 是一类重要的稀磁半导体, 在未来的自旋电子学有潜在应用[45~49].

二维掺杂TMDs一般可以通过3种方法获得, 分别是机械剥离法[16]、化学气相沉积法(CVD)[17]、物理气相沉积法(PVD)[15]. 其中, 机械剥离法要先获得均匀掺杂的单晶体材料, 可以通过化学气相输运法(CVT)获得. 在CVT方法中, 源区的温度要比生长区的温度高, 同时真空封管里面一般会有I_2或Br_2等充当载气, 物质会由气态从源区不断地输运到生长区. CVT方法不但重复性强, 而且获得的样品结晶度高. 在CVD和PVD中, 生长温度和各种源的浓度是非常重要的, 并且这两种方法对于制备大尺寸二维材料

是非常有效的, 但是, 他们对条件比较敏感, 重复性不如CVT. 合成二维掺杂TMDs难点在于, 掺杂后的材料比纯材料稳定性差, 所以异质原子更难掺杂, 尤其是原子层厚度的二维TMDs合金. CVD和PVD结合的一种方法对于合成二维TMDs掺杂材料也是十分有效的: 通过PVD使异质原子掺杂到源材料中, 然后通过CVD生长获得原子层厚度的二维掺杂TMDs材料[50].

使用MoO_3和Co_3O_4分别作为Mo和Co源, 用CVD法制备了双层Co掺杂的MoS_2($Co_{0.16}Mo_{0.84}S_2$)纳米片(图3(a))[39]. 通过拉曼图像测试, 表明Co原子主要掺杂在纳米片的边缘(图3(c)), 而且从边缘到中间逐渐减少. 通过调整初始硫的含量来控制硫的蒸气浓度, 发现硫的蒸气浓度对纳米片的形貌有影响. 随着硫的浓度的增加, 纳米片会由David形状变成规则的六边形(图3(d)), 这可能是硫的浓度影响了Co原子和Mo, S原子的亲和性. 同时, 提高生长温度, 发现CoS_2颗粒会在纳米片的边缘聚集, 然后扩展至整个纳米片, 最终成为CoS_2/MoS_2六边形结构, 电学测试表明$Co_{0.16}Mo_{0.84}S_2$显示n型, 开关比与纯MoS_2相比, 有所下降(图3(e)和(f)), 而CoS_2则是半金属, 电导很高(图3(g)). 理论研究表明, 在二维材料中, 磁性原子掺杂浓度越高, 就有可能产生高居里温度的稀磁半导体[46], 在我们制备的这种双层Co掺杂的MoS_2纳米片中, Co的浓度是比较高的, 因此这种纳米片在未来的磁性半导体领域有应用潜力.

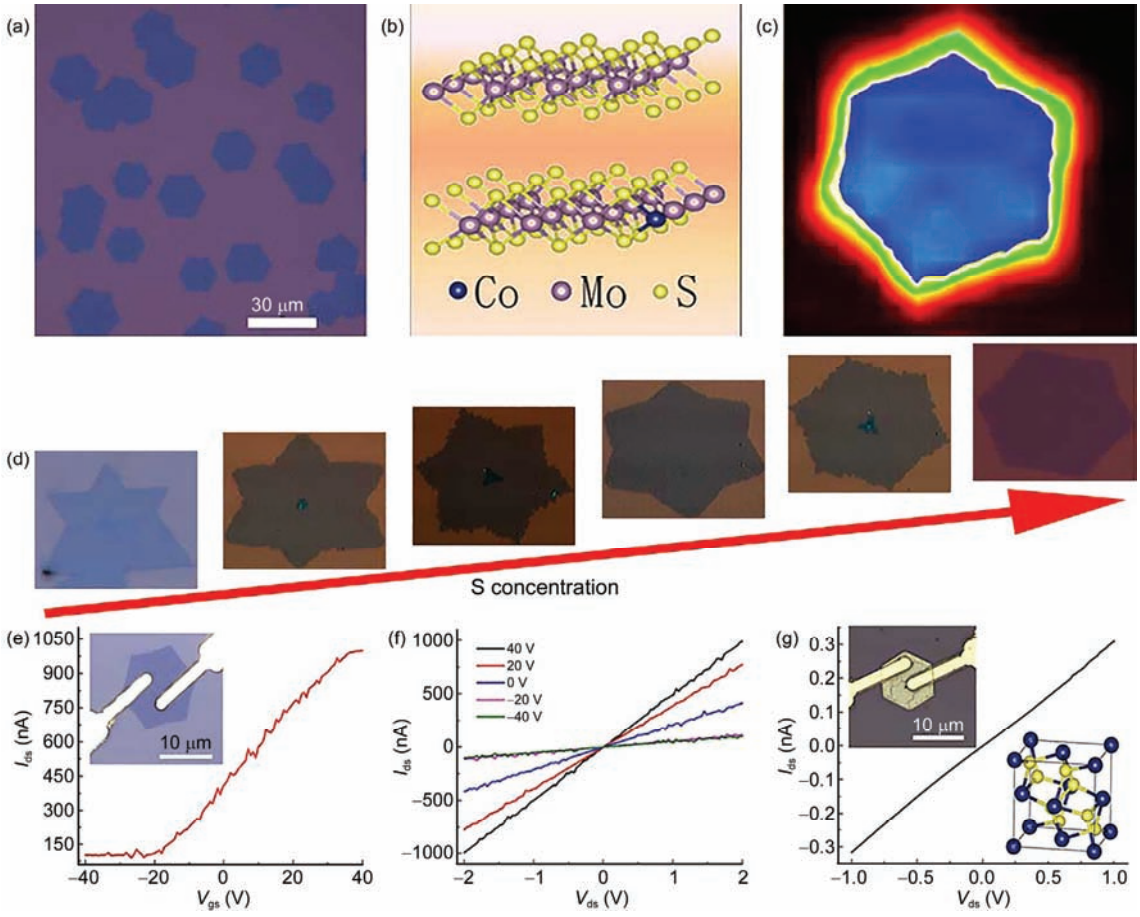

图 3 (网络版彩色)$Co_{0.16}Mo_{0.84}S_2$纳米片的表征, 生长过程及电学性能分析. (a) $Co_{0.16}Mo_{0.84}S_2$纳米片的光学显微镜图; (b) Co掺杂MoS_2原子结构图; (c) $Co_{0.16}Mo_{0.84}S_2$纳米片的拉曼图像; (d) 硫浓度对生长纳米片形貌影响; (e) $Co_{0.16}Mo_{0.84}S_2$纳米片的转移曲线; (f) $Co_{0.16}Mo_{0.84}S_2$纳米片的输出曲线; (g) CoS_2膜的*I-V*曲线

Figure 3 (Color online) Characterization, growing process and electronic property of $Co_{0.16}Mo_{0.84}S_2$ nanosheets. (a) Optical image of $Co_{0.16}Mo_{0.84}S_2$ nanosheets; (b) atomic structure of Co doped MoS_2; (c) Raman mapping of $Co_{0.16}Mo_{0.84}S_2$ nanosheets; (d) the morphology of $Co_{0.16}Mo_{0.84}S_2$ nanosheets affected by S concentration; (e) transfer characteristics of the $Co_{0.16}Mo_{0.84}S_2$ nanosheet; (f) output curves of the $Co_{0.16}Mo_{0.84}S_2$ nanosheet; (g) *I-V* curve for the CoS_2 film at room temperature

3 SnS_2/MoS_2异质结的制备及光电性能研究

由不同的半导体材料形成的异质结在现代半导体领域扮演重要的角色，他们是构建现代电子器件的重要基石. 在半导体异质结的界面处，两种材料的电子能带结构会由于静电作用而发生相应的变化. 半导体异质结在现实生活中有很多应用，比如太阳能电池、半导体激光器和发光二极管等. 二维TMDs具有独特的光学带隙结构，尤其是单层的TMDs大部分是直接带隙，同时他们还具有强烈的光与物质作用[8]. TMDs体材料的层与层之间是以较弱的范德华力连接，这样使得他们容易分离变成二维材料，同时不同的二维半导体材料垂直堆叠形成异质结时，可以不用考虑晶格匹配问题[28].

由于层状材料的机械剥离和转移技术的快速发展，机械剥离出的多种二维材料已经被人工堆叠成不同的垂直二维异质结[24]. 这些异质结的堆叠顺序和两种材料的界面对于他们的光电性能有重要影响，比如，石墨烯在SiO_2衬底上的迁移率不高，主要是由于SiO_2衬底的电荷杂质、粗糙的表面和SiO_2的光学声子等造成的散射导致的，而当通过机械堆叠的方法，把石墨烯转移到h-BN上面时，由于BN衬底具有原子级的平整度，同时没有电荷俘获，所以对于石墨烯而言，这是一种极好的衬底，这时候测出的迁移率比在SiO_2上测出来的要高1个数量级[6]. 机械堆叠法对构建任意的二维异质结提供一种最简单的方法. 然而，这些异质结的界面处的质量是有待提高的，因为他们很容易被用于转移残留的化学溶剂污染，这也是目前一直存在尚未解决的问题. 虽然剥离技术能获得高质量的二维材料，用于基础研究，但是它对于所制备出的异质结的局部、层数和界面等的控制还是远远不够的，这就阻碍了它在实际应用中的发展. 最近，化学气相沉积法(CVD)作为很有潜力制备大面积二维TMDs材料的方法受到人们的关注，在实验上，CVD法已经合成出了垂直和水平类型的异质结[51,52]. 用CVD可以在一个二维材料上面生长另一个. 原则上，直接生长二维异质结会产生表面很干净的异质结. 由于二维材料是以范德华力结合的，所以，生长的时候不用考虑晶格失配度. 理论预言和部分实验证实，具有Ⅱ型能带结构的二维范德华异质结会促进电子空穴分离，从而在光学和电学的应用上有巨大的潜能[29].

用直接气相生长法获得了外延的垂直SnS_2/MoS_2异质结，该异质结具有很大的带阶及Ⅱ型能带结构[40]. 垂直堆叠SnS_2/MoS_2异质结的形貌通过扫描电子显微镜(SEM)和原子力显微镜(AFM)表征，如图4(a)和(b)所示，我们获得的样品的产量是很高的，在靠近SnO源的部分，约为70%，其余的全是纯的MoS_2. 在该异质结中，底部是MoS_2三角形层，顶部是三角或六边形的SnS_2，AFM图像表明MoS_2层的厚度是0.73 nm，而SnS_2层的厚度是0.79 nm (图4(c)). 这表明SnS_2/MoS_2异质结是由MoS_2和SnS_2单层构成的. 图4(d)的拉曼图像进一步表明了该异质结的垂直结构. 图4(e)中表明，单层的MoS_2的PL峰强要比异质结区域高，在异质结区域出现强烈的PL淬灭，这表明MoS_2激发的很多电子转移到了更低能态的SnS_2中，而不是在MoS_2内部复合发光. 这也进一步表明该异质结的界面干净，样品质量高. 高分辨透射电子显微镜(HRTEM)展示SnS_2/MoS_2异质结区域有明显的莫尔图案(图4(f)). 长程的莫尔超晶格图案来自于空间变化的层间耦合和电子基态势能. 该SnS_2/MoS_2异质结的场效应晶体管(FETs)展示了高达27.6 cm^2(V s)的迁移率和10^6的开关比(图4(g)和(h)). 最大的光响应度是1.36 A W^{-1}，具有光伏效应(图4(i)). 制备这种具有独特光电性能的二维范德华异质结为高性能功能型电子光电器件开辟道路.

4 结论和展望

二维材料的研究是当前的一个研究热点，很多的二维材料都展现了体材料所不具备的性能. 本文介绍了我们发展出的光刻图形转移技术，以及化学气相法制备的$Co_{0.16}Mo_{0.84}S_2$掺杂二维材料，还有化学气相法直接制备的二维硫化锡/硫化钼(SnS_2/MoS_2)双层垂直异质结.

在未来的研究中，二维材料还有很多未知领域需要探索，还有很多难题需要攻克：(1) 寻找高迁移率、有实用价值的二维材料，如最近诺贝尔奖Geim组报道了高迁移率的InSe二维原子晶体[53]. 因为二维材料是原子层厚度，在微纳器件领域可以忽略短沟道效应，这样能做出高性能、超小尺寸的器件. (2) 探究二维材料的新性能. 目前二维材料的光学和电学性能研究的较多，而力学、磁性等研究的较少，有待进一步研究. (3) 摸索大面积、高质量的二维材料的生长，为二维材料的工业化应用铺平道路.

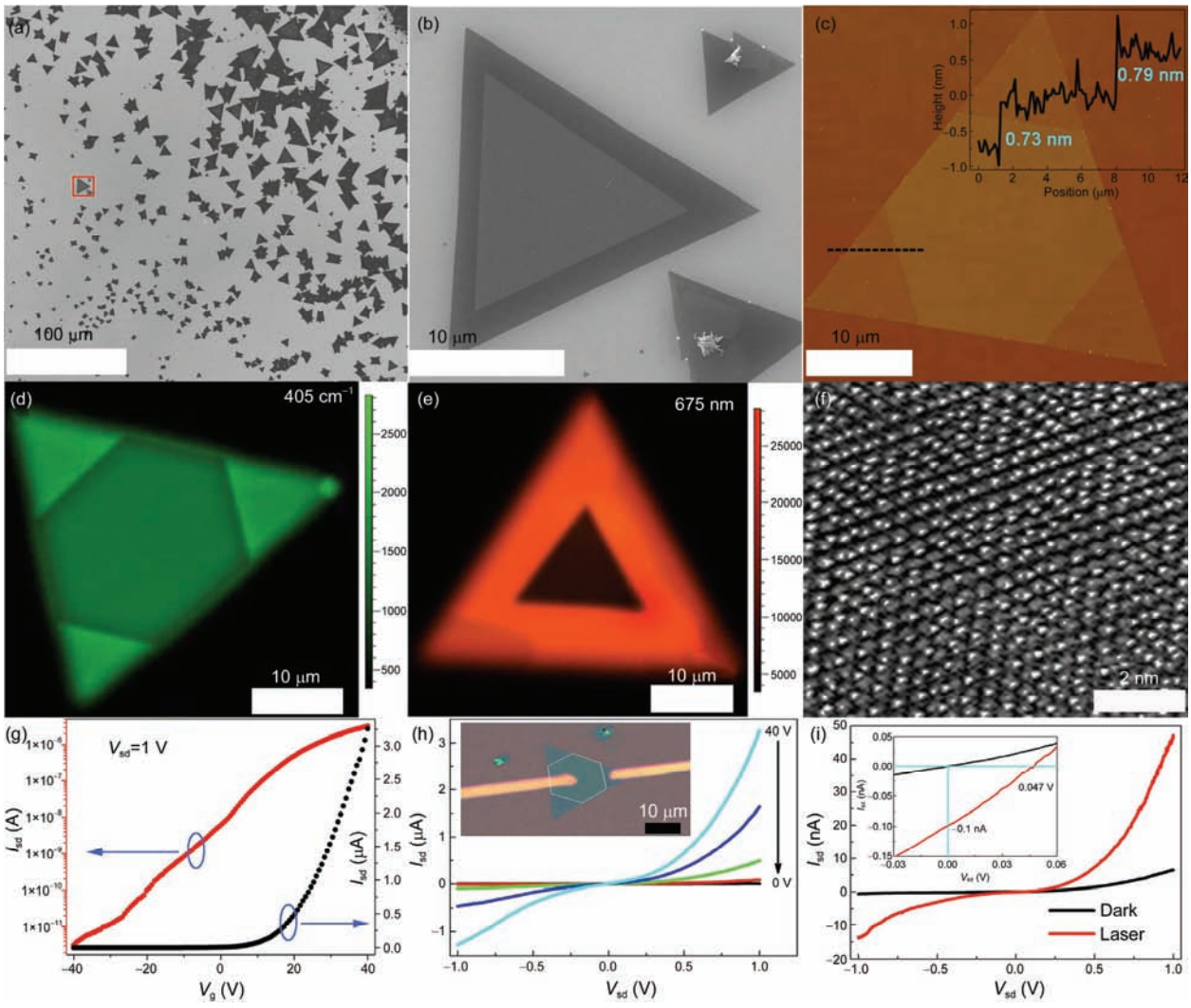

图 4 (网络版彩色)SnS_2/MoS_2异质结的表征及光电性能. (a) SnS_2/MoS_2异质结的SEM图; (b) 在(a)中标注方框的放大SEM图; (c) SnS_2/MoS_2异质结的AFM图; (d) SnS_2/MoS_2异质结在 405 cm^{-1}处拉曼图像; (e) SnS_2/MoS_2异质结在 675 nm处PL图像; (f) SnS_2/MoS_2异质结的HRTEM图; (g)和(h)分别是异质结的转移和输出曲线; (i) SnS_2/MoS_2异质结在无光照和有光照情况下的输出曲线

Figure 4 (Color online) Characterization and optoelectronic property of SnS_2/MoS_2 heterostructures. (a) SEM image of SnS_2/MoS_2 heterostructure; (b) the enlarge SEM image in (a); (c) AFM image of SnS_2/MoS_2 heterostructure; (d) Raman mapping of SnS_2/MoS_2 heterostructure at 405 cm^{-1}; (e) PL mapping of SnS_2/MoS_2 heterostructure at 675 nm; (f) HRTEM image of SnS_2/MoS_2 heterostructure; (g) transfer and (h) output characteristics of SnS_2/MoS_2 heterostructures; (i) output (I_{sd}-V_{sd}) characteristics of the heterostructure in the dark and under illumination

参考文献

1 Novoselov K S, Geim A K, Morozov S V, et al. Electric field effect in atomically thin carbon films. Science, 2004, 306: 666–669

2 Chhowalla M, Shin H S, Eda G, et al. The chemistry of two-dimensional layered transition metal dichalcogenide nanosheets. Nat Chem, 2013, 5: 263–275

3 Xia C, Li J. Recent advances in optoelectronic properties and applications of two-dimensional metal chalcogenides. J Semicond, 2016, 37: 051001

4 Tao L, Wang D, Jiang S, et al. Fabrication techniques and applications of flexible graphene-based electronic devices. J Semicond, 2016, 37: 041001

5 Tan C, Zhang H. Two-dimensional transition metal dichalcogenide nanosheet-based composites. Chem Soc Rev, 2015, 44: 2713–2731

6 Allen M J, Tung V C, Kaner R B. Honeycomb carbon: A review of graphene. Chem Rev, 2010, 110: 132–145

7 Yin Z, Li H, Li H, et al. Single-layer MoS_2 phototransistors. ACS Nano, 2012, 6: 74–80

8 Mak K F, Lee C, Hone J, et al. Atomically thin MoS_2: A new direct-gap semiconductor. Phys Rev Lett, 2010, 105: 136805

9 Li B, Yang S, Huo N, et al. Growth of large area few-layer or monolayer MoS_2 from controllable MoO_3 nanowire nuclei. RSC Adv, 2014, 4: 26407–26412

10 Li Y, Huang L, Li B, et al. Co-nucleus 1D/2D heterostructures with Bi_2S_3 nanowire and MoS_2 monolayer: One-step growth and defect-induced formation mechanism. ACS Nano, 2016, 10: 8938–8946

11 Wang P, Nan R, Jian Z. The effects of deep-level defects on the electrical properties of $Cd_{0.9}Zn_{0.1}Te$ crystals. J Semicond, 2017, 38: 062002

12 Wang Q H, Kalantar-Zadeh K, Kis A, et al. Electronics and optoelectronics of two-dimensional transition metal dichalcogenides. Nat Nanotech, 2012, 7: 699–712

13 Li B, Huang L, Zhao G, et al. Large-size 2D β-Cu_2S nanosheets with giant phase transition temperature lowering (120 K) synthesized by a novel method of super-cooling chemical-vapor-deposition. Adv Mater, 2016, 28: 8271–8276

14 Feng Q, Mao N, Wu J, et al. Growth of $MoS_{2(1-x)}Se_{2x}$ (x=0.41–1.00) monolayer alloys with controlled morphology by physical vapor deposition. ACS Nano, 2015, 9: 7450–7455

15 Feng Q L, Zhu Y M, Hong J H, et al. Growth of large-area 2D $MoS_{2(1-x)}Se_{2x}$ semiconductor alloys. Adv Mater, 2014, 26: 2648–2653

16 Tongay S, Narang D S, Kang J, et al. Two-dimensional semiconductor alloys: Monolayer $Mo_{1-x}W_xSe_2$. Appl Phys Lett, 2014, 104: 012101

17 Li H, Duan X, Wu X, et al. Growth of alloy $MoS_{2x}Se_{2(1-x)}$ nanosheets with fully tunable chemical compositions and optical properties. J Am Chem Soc, 2014, 136: 3756–3759

18 Li H, Zhang Q, Duan X, et al. Lateral growth of composition graded atomic layer $MoS_{2(1-x)}Se_{2x}$ nanosheets. J Am Chem Soc, 2015, 137: 5284–5287

19 Chen Y, Dumcenco D O, Zhu Y, et al. Composition-dependent Raman modes of $Mo_{1-x}W_xS_2$ monolayer alloys. Nanoscale, 2014, 6: 2833–2839

20 Liu H, Antwi K K A, Chua S, et al. Vapor-phase growth and characterization of $Mo_{1-x}W_xS_2$ ($0<x<1$) atomic layers on 2-inch sapphire substrates. Nanoscale, 2014, 6: 624–629

21 Chen Y, Xi J, Dumcenco D O, et al. Tunable band gap photoluminescence from atomically thin transition-metal dichalcogenide alloys. ACS Nano, 2013, 7: 4610–4616

22 Liu S, Huang L, Wu K, et al. Tuned polarity and enhanced optoelectronic performances of few-layer $Nb_{0.125}Re_{0.875}Se_2$ flakes. Appl Phys Lett, 2016, 109: 112102

23 Yang S, Wang C, Ataca C, et al. Self-driven photodetector and ambipolar transistor in atomically thin GaTe-MoS_2 p-n vdW heterostructure. ACS Appl Mater Interfaces, 2016, 8: 2533–2539

24 Huo N J, Kang J, Wei Z M, et al. Novel and enhanced optoelectronic performances of multilayer MoS_2-WS_2 heterostructure transistors. Adv Funct Mater, 2014, 24: 7025–7031

25 Kang J, Li J, Li S S, et al. Electronic structural Moiré pattern effects on MoS_2/$MoSe_2$ 2D heterostructures. Nano Lett, 2013, 13: 5485–5490

26 Huang C, Wu S, Sanchez A M, et al. Lateral heterojunctions within monolayer $MoSe_2$-WSe_2 semiconductors. Nat Mater, 2014, 13: 1096–1101

27 Hong X, Kim J, Shi S F, et al. Ultrafast charge transfer in atomically thin MoS_2/WS_2 heterostructures. Nat Nanotech, 2014, 9: 682–686

28 Geim A K, Grigorieva I V. Van der Waals heterostructures. Nature, 2013, 499: 419–425

29 Li Y M, Li J, Shi L K, et al. Light-induced exciton spin Hall effect in van der Waals heterostructures. Phys Rev Lett, 2015, 115: 166804

30 Yang J, Huo N, Li Y, et al. Gate-tunable ultra-high photoresponsivity of 2D heterostructures based on few layer MoS_2 and solution-processed rGO. Adv Electron Mater, 2015, 1: 1500267

31 Huang L, Huo N, Li Y, et al. Electric-field tunable band offsets in black phosphorus and MoS_2 van der Waals p-n heterostructure. J Phys Chem Lett, 2015, 6: 2483–2488

32 Huang L, Li Y, Wei Z, et al. Strain induced piezoelectric effect in black phosphorus and MoS_2 van der Waals heterostructure. Sci Rep, 2015, 5: 16448

33 Huo N, Yang J, Huang L, et al. Tunable polarity behavior and self-driven photoswitching in p-WSe_2/n-WS_2 heterojunctions. Small, 2015, 11: 5430–5438

34 Li Y, Wang Y, Huang L, et al. Anti-ambipolar field-effect transistors based on few-layer 2D transition metal dichalcogenides. ACS Appl Mater Interfaces, 2016, 8: 15574–15581

35 Wang X, Huang L, Peng Y, et al. Enhanced rectification, transport property and photocurrent generation of multilayer $ReSe_2$/MoS_2 p-n heterojunctions. Nano Res, 2016, 9: 507–516

36 Tang K, Gu S, Ye J, et al. High-quality ZnO growth, doping, and polarization effect. J Semicond, 2016, 37: 031001

37 Li J M, Liu Z, Liu Z Q, et al. Advances and prospects in nitrides based light-emitting-diodes. J Semicond, 2016, 37: 061001

38 Li Y, Huang L, Zhong M, et al. An efficient and low-cost photolithographic-pattern-transfer technique to fabricate electrode arrays for micro-/nanoelectronics. Adv Mater Tech, 2016, 1: 1600001

39 Li B, Huang L, Zhong M, et al. Synthesis and transport properties of large-scale alloy $Co_{0.16}Mo_{0.84}S_2$ bilayer nanosheets. ACS Nano, 2015, 9: 1257–1262

40 Li B, Huang L, Zhong M, et al. Direct vapor phase growth and optoelectronic application of large band offset SnS_2/MoS_2 vertical bilayer heterostructures with high lattice mismatch. Adv Electron Mater, 2016, 2: 1600298

41 Liu Y, Weiss N O, Duan X, et al. Van der Waals heterostructures and devices. Nat Rev Mater, 2016, 1: 16042

42 Suh J, Park T E, Lin D Y, et al. Doping against the native propensity of MoS_2: Degenerate hole doping by cation substitution. Nano Lett, 2014, 14: 6976–6982

43 Perumal P, Ulaganathan R K, Sankar R, et al. Ultra-thin layered ternary single crystals $Sn(S_xSe_{1-x})_{(2)}$ with bandgap engineering for high performance phototransistors on versatile substrates. Adv Funct Mater, 2016, 26: 3630–3638

44 Wang Y, Huang L, Li B, et al. Composition-tunable 2D $SnSe_{2(1-x)}S_{2x}$ alloys towards efficient bandgap engineering and high performance (opto)electronics. J Mater Chem C, 2017, 5: 84–90

45 Sun L, Zhou W, Liang Y, et al. Magnetic properties in Fe-doped SnS_2: Density functional calculations. Comp Mater Sci, 2016, 117: 489–495

46 Cheng Y C, Zhu Z Y, Mi W B, et al. Prediction of two-dimensional diluted magnetic semiconductors: Doped monolayer MoS_2 systems. Phys Rev B, 2013, 87: 100401

47 Mishra R, Zhou W, Pennycook S J, et al. Long-range ferromagnetic ordering in manganese-doped two-dimensional dichalcogenides. Phys Rev B, 2013, 88: 144409

48 Ramasubramaniam A, Naveh D. Mn-doped monolayer MoS_2: An atomically thin dilute magnetic semiconductor. Phys Rev B, 2013, 87: 195201

49 Seixas L, Carvalho A, Castro N A H. Atomically thin dilute magnetism in Co-doped phosphorene. Phys Rev B, 2015, 91: 155138

50 Bai G, Yuan S, Zhao Y, et al. 2D layered materials of rare-earth Er-doped MoS_2 with NIR-to-NIR down- and up-conversion photoluminescence. Adv Mater, 2016, 28: 7472–7477

51 Gong Y, Lin J, Wang X, et al. Vertical and in-plane heterostructures from WS_2/MoS_2 monolayers. Nat Mater, 2014, 13: 1135–1142

52 Duan X, Wang C, Shaw J C, et al. Lateral epitaxial growth of two-dimensional layered semiconductor heterojunctions. Nat Nanotech, 2014, 9: 1024–1030

53 Bandurin D A, Tyurnina A V, Yu G L, et al. High electron mobility, quantum Hall effect and anomalous optical response in atomically thin InSe. Nat Nanotech, 2017, 12: 223–228

Summary for “二维半导体材料的生长和光电性能研究”

Growth and optoelectronic property of two-dimensional semiconductors

LI Bo & WEI ZhongMing*

State Key Laboratory of Superlattices and Microstructures, Institute of Semiconductors, Chinese Academy of Sciences, Beijing 100083, China
* Corresponding author, E-mail: zmwei@semi.ac.cn

Two-dimensional (2D) nanosheets of layered transition metal dichalcogenides (TMDs) have received significant attention because some of them are semiconductors with sizable band gaps and are naturally abundant. Here, we report the photolithographic-pattern transfer (PPT) technology used to fabricate FETs of two-dimensional materials. To explore the electrical properties and realize functional optoelectronics and electronics from semiconductors, the fabrication of devices (such as field-effect transistors (FET), diodes and Hall bars) and integrated circuits is necessary and important. An essential step in fabricating micro-/nanoelectronics is making the metal electrode arrays. Such a PPT method can be used to efficiently design and prepare complicated electrode arrays for electronics and optoelectronics, and is especially suitable for 2D materials. Few-layer MoS_2 made by electron beam lithography (EBL), gold-wire mask moving (GWM), and this method are used as templates for comparison. The mobility of our thin MoS_2 flake is comparable to the results of devices from EBL and better than the results of the GWM method. Further complicated device applications such as a top-gate FET, a Hall bar, and heterostructure transistors could also be easily realized based on such a method. We also report the growth and electric transport of Co doped MoS_2 bilayer. As the initial loading of the sulfur increases, the morphology of the $Co_xMo_{1-x}S_2$ ($0<x<1$) nanosheets becomes hexagons from David stars step by step at 680°C. We find that Co atoms mainly distribute at the edge of nanosheets. When the temperature increases from 680 to 750°C, high-quality cubic pyrite-type crystal structure CoS_2 grows on the surface of $Co_xMo_{1-x}S_2$ nanosheet gradually and forms hexagonal film induced by the nanosheet. Electrical transport measurements reveal that the $Co_xMo_{1-x}S_2$ nanosheets and CoS_2 films exhibit n-type semiconducting transport behavior and half-metallic behavior, respectively. Theoretical calculations of their band structures agree well with the experimental results. These alloy nanosheets of $Co_xMo_{1-x}S_2$ should have large potential applications in the tunable optoelectronics. Then, we report the vapor phase growth and optoelectronic property of vertical bilayer SnS_2/MoS_2 heterostructure. 2D van der Waals heterostructures with different types of band alignment have recently attracted great attention due to their unique optical and electrical properties. Most 2D heterostructures are formed by transfer-stacking two monolayers together, but the interfacial quality and controllable orientation of such artificial structures are inferior to those epitaxial grown heterostructures. An extremely Type II band alignment exists in this 2D heterostructure, with band offset larger than any other reported. Consistent with the large band offset, distinctive optical properties including strong photoluminescence quenching in the heterostructure area are observed in the heterostructure. The SnS_2/MoS_2 heterostructures also exhibit well-aligned lattice orientation between the two layers, forming a periodic Moiré superlattice pattern with high lattice mismatch. Electrical transport and photoresponsive studies demonstrate that the SnS_2/MoS_2 heterostructures exhibit an obvious photovoltaic effect and possess high on/off ratio ($>10^6$), high mobility (27.6 $cm^2\ V^{-1}\ s^{-1}$) and high photoresponsivity (1.36 A W^{-1}). Efficient synthesis of such vertical heterostructure may open up new realms in 2D functional electronics and optoelectronics. Finally we give some perspectives on studies of two-dimensional materials in future.

two-dimensional materials, MoS_2, vapor phase growth, electric transport

doi: 10.1360/N972017-00431